

Resonant Lifetime of Core-Excited Organic Adsorbates from First Principles

Guido Fratesi,^{*,†,||} Carlo Motta,[‡] Mario Italo Trioni,[¶] Gian Paolo Brivio,[‡] and Daniel
Sánchez-Portal^{§,⊥}

*ETSF, CNISM, Dipartimento di Fisica, Università degli Studi di Milano, via Celoria 16, I-20133
Milano, Italy, Dipartimento di Scienza dei Materiali, Università di Milano-Bicocca, via Cozzi 55,
I-20125 Milano, Italy, CNR-National Research Council of Italy, ISTM, Via Golgi 19, I-20133
Milano, Italy, and Centro de Física de Materiales CSIC-UPV/EHU, Paseo Manuel de Lardizabal
5, 20018 San Sebastián, Spain*

E-mail: guido.fratesi@unimi.it

^aCurrent address: School of Physics and CRANN, Trinity College, Dublin 2, Ireland

^{*}To whom correspondence should be addressed

[†]ETSF, CNISM, Dipartimento di Fisica, Università degli Studi di Milano, via Celoria 16, I-20133 Milano, Italy

[‡]Dipartimento di Scienza dei Materiali, Università di Milano-Bicocca, via Cozzi 55, I-20125 Milano, Italy

[¶]CNR-National Research Council of Italy, ISTM, Via Golgi 19, I-20133 Milano, Italy

[§]Centro de Física de Materiales CSIC-UPV/EHU, Paseo Manuel de Lardizabal 5, 20018 San Sebastián, Spain

^{||}Dipartimento di Scienza dei Materiali, Università di Milano-Bicocca, via Cozzi 55, I-20125 Milano, Italy

[⊥]Donostia International Physics Center (DIPC), Paseo Manuel de Lardizabal 4, 20018 San Sebastián, Spain

Abstract

We investigate by first-principles simulations the resonant electron-transfer lifetime from the excited state of an organic adsorbate to a semiconductor surface, namely isonicotinic acid on rutile $\text{TiO}_2(110)$. The molecule-substrate interaction is described using density functional theory, while the effect of a truly semi-infinite substrate is taken into account by Green's function techniques. Excitonic effects due to the presence of core-excited atoms in the molecule are shown to be instrumental to understand the electron-transfer times measured using the so-called core-hole-clock technique. In particular, for the isonicotinic acid on $\text{TiO}_2(110)$, we find that the charge injection from the LUMO is quenched since this state lies within the substrate band gap. We compute the resonant charge-transfer times from LUMO+1 and LUMO+2, and systematically investigate the dependence of the elastic lifetimes of these states on the alignment among adsorbate and substrate states.

Keywords: Dye sensitized solar cells; Organic electronics; Charge-transfer dynamics; Resonant spectroscopy; Density functional theory

Introduction

Charge transfer from an electronically excited adsorbed molecule is a process with wide relevance in several fields such as surface reaction dynamics, photocatalysis, molecular electronics and organic photovoltaics. Regarding the last topic, dye sensitized solar cells (DSSC) are an important emergent technology providing new ways to harvest energy from light.¹⁻⁴ They are typically constituted by a transition metal complex or an organic dye adsorbed on an insulating substrate, which in most cases is TiO_2 or ZnO . Light radiation excites an electronic transition within the adsorbate, usually involving the highest occupied molecular orbital (HOMO), and the excited electron may be transferred to the continuum of states in the conduction band of the substrate. The oxidized dye is then restored to its reduced form by a redox pair in solution, and a photocurrent can be generated in the circuit. The relative time scales of these processes are fundamental for the cell to work properly. In particular, the first step, i.e., the transfer of the excited electron to the anode, must be faster

than charge recombination within the molecule so the electron can be injected to the surface and quickly delocalize into the bulk. In this way, the importance of the recombination channel within the molecule is reduced and the produced electron and hole can be efficiently separated.

Unoccupied levels and electron charge-transfer dynamics at surfaces can be investigated by a variety of experimental techniques like resonant core-level electron spectroscopy,^{5–7} two-photon photoemission and other femtosecond pump-probe time-resolved (PPTR) laser spectroscopies,^{8–10} and inverse photoemission spectroscopy (IPS).^{11–13} In the first method, also named core-hole-clock spectroscopy, a shallow core level of the absorbed molecule is photoexcited by X-ray absorption (XAS) into an unoccupied bound state of the adsorbate. The photoexcited electron is eventually injected to the substrate, while the decay of the excited core usually proceeds via an Auger decay. The Auger electron can be emitted before or after the photoexcited electron (sometimes referred to as spectator electron) is transferred to the surface. From the relative intensities of these two Auger decay channels, the charge-transfer time of the initially excited electron can be obtained in units of the Auger decay time. This technique has the advantage to access the fastest timescales (down to the attosecond¹⁴), but the core hole produces a significant perturbation to the valence electronic structure. For this reason, unoccupied states might significantly differ from that of the molecule excited from more extended molecular orbitals (MOs), like the HOMO. For example, the lowest unoccupied molecular orbital (LUMO) of bi-isonicotinic and isonicotinic acid on rutile TiO₂(110) has been found to lie in the substrate gap in XAS experiments, since it is lowered by the attractive potential due to the core-hole localized in the nitrogen atom.¹⁵ Still, electron transfer times of a few femtoseconds could be measured for the next two higher resonances that overlap with the conduction band.^{15,16} Another indication of the strong modification of the molecular electronic structure is due to the fact that, even in relatively small molecules like paracyclophanes, charge transfer times measured by core-hole-clock spectroscopy strongly depend on the site of the core excitation.¹⁷

Given the complexity of the dye-substrate system, density functional theory (DFT) is most often the method of choice for the theoretical description of its electronic structure, while the

nuclei are described classically. Within DFT, different approaches were proposed to study some of the various aspects of the electron injection process.^{18,19} Estimates of adiabatic and non-adiabatic contributions were accomplished by coupled electron/ion dynamics at various temperatures^{20,21} or calculation of phonon self-energies,²² while electron-electron contributions have also been found to be dominant in some cases.²³ Other methods focus instead on the resonant electron transfer which operates for molecular states well within the energy continuum of the substrate bands.^{2,18,24}

Albeit cluster^{25–27} or slab^{2,19,28} models are commonly adopted, a truly continuum density of states, without artificial confinement effects, is only reached for a substrate which extends semi-infinately also in the direction perpendicular to the surface.²⁹ Several methods have been proposed over the years to deal with calculations involving semi-infinite substrates. Among them, one of the most powerful is probably the so-called embedding technique,^{29–31} which allows performing calculations of the surface Green’s function where only a few atomic layers closer to the surface are taken into account explicitly. Using this method, the elastic lifetimes of adsorbed molecules on metals have been calculated with great accuracy.^{32,33} Unfortunately, in practice the implementation of embedding can be quite cumbersome and, in many cases, it is restricted to deal with particular geometries that allow performing necessary simplifications. This has probably prevented a wider application of this method so far. Most approaches to date also neglect the strong interaction of the valence states with the core-hole, even when trying to account for experimental results obtained by the core-hole-clock method. These two relevant problems need a more careful theoretical treatment.

In this paper, we would like to contribute along these research lines. In particular, we calculate the resonant lifetimes of core-excited organic species, focusing on isonicotinic acid adsorbed on rutile $\text{TiO}_2(110)$ as a relevant example, and compare them with the experimental information from core-hole-clock spectroscopy at the N K-edge.¹⁶ To deal with a semi-infinite substrate we use here a Green’s function procedure similar to that used by one of us to study resonant charge-transfer from simple adsorbates.^{34,35} We show that such methodology can be easily extended to treat more complex adsorbates, and different types of substrates, using the plethora of available

techniques for the first-principles description of quantum transport in nanostructures.^{36–39} We also deal with the core hole in the adsorbate, and the resulting excitonic effects. Given the large degree of localization of the core hole, one can treat the electron-hole interaction statically by relaxing the electronic structure in the presence of a core-to-valence excitation.^{15,25,40,41} In this way we can account for the large relaxations of some of the MOs induced by the presence of the localized hole, as well as the associated changes in the MO energies relative to the substrate bands.

Method

We now describe an *ab initio* method to evaluate the resonant lifetime of the MOs of molecules adsorbed at the surface of a semi-infinite crystal. We adopt a Green’s function formalism within DFT^{34,35} and setup the problem in analogy to the study of quantum conductance through molecular junctions. Here we make use of the SIESTA/TranSIESTA packages,^{36,42} but we would like to remind that the procedure below is easily realized using other quantum-transport codes. We form a fictitious molecular junction as shown in Fig. 1 and assume that the space is divided into three regions: two semi-infinite “electrodes” and a central “contact” region. The contact region contains two identical copies of the surface under study and includes a vacuum portion large enough to decouple the left and right adsorbates. Notice that, although not strictly necessary, it is advisable to choose a symmetric setup like the one depicted in Fig. 1 for reasons outlined below. The Green’s function is computed only in the contact region, upon adding to the Hamiltonian the effect of the semi-infinite substrates/electrodes using self-energy operators. These are obtained from bulk calculations of the substrate material, as usual in transport calculations.³⁶ Improving upon our previous calculations,^{34,35} restricted to combine information from Kohn-Sham (KS) Hamiltonians obtained from both bulk and slab calculations, the current scheme is implemented using quantum transport codes that can deal with finite bias drops. This allows, at least in principle, carrying out self-consistent calculations of the surface region under the open boundary conditions imposed by the presence of the semi-infinite substrate, possibly with the application of external electric fields.

The Green's function is the central quantity in our approach. In terms of the Green's function of the surface region we can, for example, compute the density of states (DOS) projected onto a wavepacket $\Phi(\mathbf{r})$ localized at the surface

$$\rho_\Phi(E) = \frac{1}{\pi} \text{Im}[G_{\Phi\Phi}(E)] = \frac{1}{\pi} \text{Im} \left[\int d\mathbf{r} \int d\mathbf{r}' \Phi^*(\mathbf{r}) G(\mathbf{r}, \mathbf{r}', E) \Phi(\mathbf{r}') \right]. \quad (1)$$

$\rho_\Phi(E)$ can be used to treat the dynamics of the population of $\Phi(\mathbf{r})$ in several ways.^{34,35} In particular, if the $\rho_\Phi(E)$ is accurately described by a single peak, its full width at half maximum (FWHM) Γ can be used to obtain a good estimation of the resonant lifetime of the initial wavepacket $\Phi(\mathbf{r})$ as $\tau = \hbar/\Gamma$.^{34,43}

Observe that our system is periodic along the in-plane directions. Therefore, the Green's function of the full adsorbate/substrate system can be expressed as

$$G(\mathbf{r}, \mathbf{r}', E) = \frac{1}{N_{\mathbf{k}_\parallel}} \sum_{\mathbf{k}_\parallel} \sum_{\mu\nu} G_{\mathbf{k}_\parallel}^{\mu\nu}(E) \phi_{\mu\mathbf{k}_\parallel}(\mathbf{r}) \phi_{\nu\mathbf{k}_\parallel}^*(\mathbf{r}'), \quad (2)$$

where \mathbf{k}_\parallel is the crystalline momentum parallel to the surface and

$$\phi_{\mu\mathbf{k}_\parallel}(\mathbf{r}) = \sum_{\mathbf{R}} e^{-i\mathbf{k}_\parallel \cdot (\mathbf{R} + \mathbf{R}_\mu)} \phi_\mu(\mathbf{r} - \mathbf{R} - \mathbf{R}_\mu) \quad (3)$$

are Bloch-like basis functions built by summing localized (atom-centered) orbitals ϕ_μ over the Bravais lattice vectors \mathbf{R} , with \mathbf{R}_μ the coordinate of the center of the μ -th orbital within the unit cell. The coefficients $G_{\mathbf{k}_\parallel}^{\mu\nu}(E)$ are evaluated from the equation

$$\sum_{\lambda} G_{\mathbf{k}_\parallel}^{\mu\lambda}(E) [H_{\lambda\nu\mathbf{k}_\parallel} - ES_{\lambda\nu\mathbf{k}_\parallel}] = \delta_V^\mu, \quad (4)$$

where $H_{\mathbf{k}_\parallel}$ and $S_{\mathbf{k}_\parallel}$ are the Hamiltonian and the overlap matrix elements between Bloch basis functions, respectively.

In our case, the relevant initial wavepacket $\Phi(\mathbf{r})$ is one of the MOs of a single adsorbate, as it occurs for a localized excitation from a core level like in core-hole-clock experiments.⁶ To

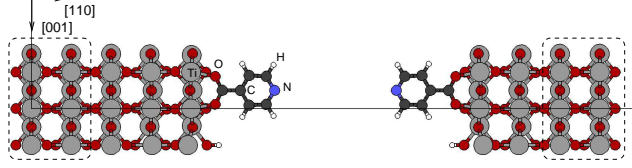


Figure 1: Side view of the model geometry for isonicotinic acid on rutile $\text{TiO}_2(110)$. The two leftmost and rightmost TiO_2 trilayers are coupled to bulk by means of self-energy operators.

avoid ambiguities, and to ensure their “molecular character”, here we use the MOs of an isolated, free-standing molecule (keeping the adsorbed geometry) as our initial wavepackets. Thus, $\Phi(\mathbf{r}) = \sum_{\mu} b^{\mu} \phi_{\mu}(\mathbf{r} - \mathbf{R}_{\mu})$, where the b^{μ} are the coefficients of the MO in the atomic orbitals belonging to that molecule. The projection of the Green’s function hence reads

$$G_{\Phi\Phi}(E) = \frac{1}{N_{\mathbf{k}_{\parallel}}} \sum_{\mathbf{k}_{\parallel}} \sum_{\lambda\mu\nu\rho} b_{\mathbf{k}_{\parallel}}^{\lambda*} S_{\lambda\mu\mathbf{k}_{\parallel}} G_{\mathbf{k}_{\parallel}}^{\mu\nu}(E) S_{\nu\rho\mathbf{k}_{\parallel}} b_{\mathbf{k}_{\parallel}}^{\rho}, \quad (5)$$

where the \mathbf{k}_{\parallel} dependence of the coefficients $b_{\mathbf{k}_{\parallel}}^{\mu} = b^{\mu} e^{i\mathbf{k}_{\parallel} \cdot \mathbf{R}_{\mu}}$ is related to the phase conventions established in Eq. (3).⁴² We notice here that Eq. (5) is equivalent to a Wannier-like transformation of the MOs in our periodic molecular overlayer $\Phi(\mathbf{r}) = \frac{1}{N_{\mathbf{k}_{\parallel}}} \sum_{\mathbf{k}_{\parallel}} \Phi_{\mathbf{k}_{\parallel}}(\mathbf{r})$, producing the same result. We observe that the width obtained from Eq. (5) as an average of Green’s functions at different \mathbf{k}_{\parallel} cannot be interpreted as the average of a \mathbf{k}_{\parallel} -dependent linewidth. In particular, there is an additional contribution in Eq. (5) due to the possible dispersion of the molecular bands within the overlayer, i.e., the energy of the MO-derived states might depend on \mathbf{k}_{\parallel} . Notice that, in the experiment, the presence of a localized core excitation should exclude this possibility. However, the use of periodic boundary conditions in our calculations makes this point relevant even in the core-excited species. This additional width is not related to charge transfer towards the substrate, but rather to hopping towards neighboring molecules, possibly mediated by the substrate. This contribution should be avoided when focusing on isolated adsorbates, as it can be done by different schemes.³⁴ Here, however, we have found that the interaction among neighboring molecules and the corresponding molecular band width is negligible. Thus, it was not necessary to correct the results obtained by Eq. (5). It is also important to stress that a sufficiently dense \mathbf{k}_{\parallel} sampling, that scales

inversely proportional to the lateral size of the supercell used in the calculations, is necessary to converge the results.

While the formalism presented so far is rather general, we hereby specify the computational details for the simulations presented in the next Section. We focus on isonicotinic acid ($\text{NC}_5\text{H}_4\text{COOH}$) adsorbed on the (110) surface of rutile TiO_2 (see Fig.1). According to the literature^{21,44–46} we take a dehydrogenated, bidentate structure with the O atoms of the molecule attached to the fivefold coordinated Ti atoms of the surface, and the aromatic ring perpendicular to the substrate. A (3×1) surface periodicity is assumed. The molecular coordinates and those of the topmost two TiO_2 trilayers were determined by relaxing a 5-trilayer slab with molecules on both sides. The junction setup is constructed by adding four TiO_2 trilayers in bulk positions to the slab, obtaining the simulation cell shown in Fig.1. The left/right subsystems are separated by a vacuum region of 10 Å. We have run DFT calculations with the Perdew-Burke-Ernzerhof⁴⁷ approximation for exchange-correlation. A (3×2) \mathbf{k}_{\parallel} mesh was adequate to determine the structural properties, while a denser (12×8) was adopted to compute Eq. (5). Structural relaxations were performed with SIESTA using a double- ζ polarized (DZP) basis set.⁴² Several tests indicated that the TranSIESTA³⁶ results for the DOS of the system were almost identical using a DZP and a smaller double- ζ (DZ) basis set for the substrate. Therefore, we finally used the DZ basis for the Green's function calculations shown below. The expansion coefficients for the MOs b^{μ} were extracted by a molecule-in-a-box calculation for the protonated species. We used a protonated molecule to preserve its closed character, although this hydrogen atom is lost upon adsorption. Fortunately, for the MOs that we considered here the contribution of this additional hydrogen atom is negligible and the corresponding coefficients (b^{μ} with $\mu \in \text{extra-H}$) can be safely neglected without significantly modifying the distribution, shape and normalization of the MOs. We evaluate the DOS projected on the molecular orbital, $\rho_{\Phi}(E)$, from the imaginary part of the Green's function determined at complex energy $E + i\gamma/2$, where γ adds to the total FWHM. So we fit the result with a lorentzian function with FWHM $\Gamma + \gamma$:

$$\rho_{\Phi}(E) \propto \frac{1}{\pi} \frac{(\Gamma + \gamma)/2}{(E - E_{\Phi})^2 + [(\Gamma + \gamma)/2]^2}, \quad (6)$$

with E_{Φ} and Γ as fitting parameters. We checked the independence of the results on γ for various cases and chose the value $\gamma = 20$ meV.

Some additional technical aspects are presented next, highlighting the differences with standard transport calculations using metallic leads. In principle, the two left/right parts of the “contact” in Fig. 1 could be different, and especially one of them could be an undecorated surface, or an empty volume. However, in the current version of SIESTA/TranSIESTA a preliminary slab calculation is needed to get the Hamiltonian matrix elements so that, the left and right part are the upper and lower portions of such a slab (with unit cell as indicated by the solid line in Fig. 1). Consequently, a symmetric configuration avoids spurious electric fields across the system. Another issue concerns the connection of the electronic potentials of the contact region with that of the bulk electrodes. The Fermi level can be chosen as a reference in a metallic system, but not in the case of a semiconductor like the one of interest here. We instead align the potential (here the planar averaged one) deep inside the slab with that of the bulk one.⁴⁸ Differently, one could also take a deep level of TiO_2 as an energy reference. No external bias is applied in the present calculations. As SIESTA uses pseudopotentials to describe core electrons, pseudopotentials for core-excited atoms⁴⁹ were generated to describe the system in presence of a N $1s^*$ atom, as it occurs in the XAS experiments that we want to address.¹⁶

Results

We start by discussing the properties of the system in the ground state, i.e., we do not introduce any explicit excitation in the system, but study the widths of the MOs in the KS spectrum corresponding to the ground state of the molecule/substrate system. The DOS projected on the gas-phase MOs ranging from the HOMO to the LUMO+2¹ is displayed in Fig. 2. The DOS of bulk TiO_2 is also shown, with the bandgap underestimated with respect to the experimental value of 3.0 eV,⁵⁰ as expected using KS-DFT with standard semilocal functionals. From lower to higher energy, we can

¹As a matter of fact, the LUMO+2 of the adsorbed system corresponds to the LUMO+3 of the gas phase molecule, since the gas phase LUMO+2 is localized at the H, eventually removed upon adsorption.

identify five features, named (a)-(e) in the figure, which are better discussed in conjunction with their real-space contribution (local DOS), integrated in small energy window (± 0.1 eV) around the main peak. Those are reported in Fig. 3(a)-(e), respectively. The HOMO (a) close to the valence

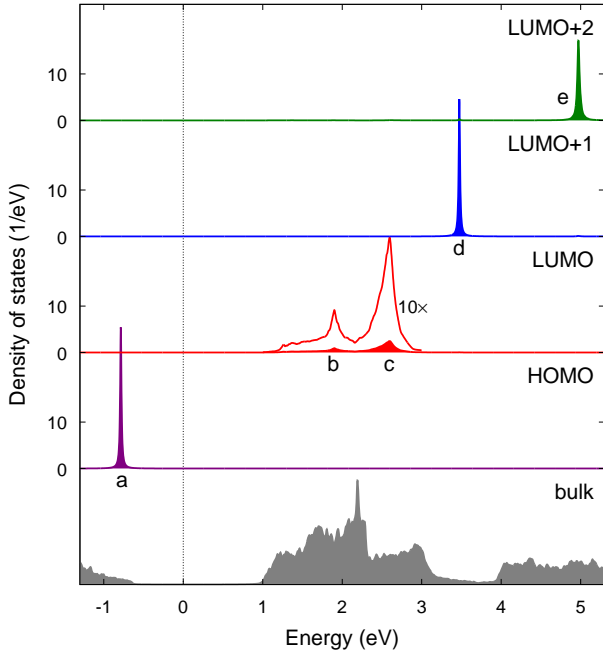


Figure 2: DOS for isonicotinic acid adsorbed on semi-infinite $\text{TiO}_2(110)$, projected on the gas-phase molecular orbitals. The shaded area is the bulk TiO_2 DOS.

band edge shows no hybridization with substrate states and its density distribution is apparently the same as in the gas phase, with no weight on the anchoring $-\text{COO}-$ group. For this state, which could be of potential interest for hole injection, we obtain $\Gamma = 0$. Conversely, the LUMO lies well within the conduction band. Here, our method shows a level of detail beyond many approaches previously developed to determine resonant charge-transfer times.² For the LUMO we identify a behavior which has been well characterized for small adsorbates with strong electronic coupling to the substrate:⁵¹ The MO splits in two components, (b) and (c), the former one with dominant adsorbate-substrate bonding character and the latter one mostly antibonding (as the analysis of nodal structure shows, see Fig. 2). Both components broaden in energy becoming resonances which extend spatially over the substrate. By fitting each peak independently, we obtain $\Gamma^{(b)} = 80$ meV and $\Gamma^{(c)} = 186$ meV, hence $\tau^{(b)} = 8$ fs for (b) and $\tau^{(c)} = 4$ fs for the most intense component

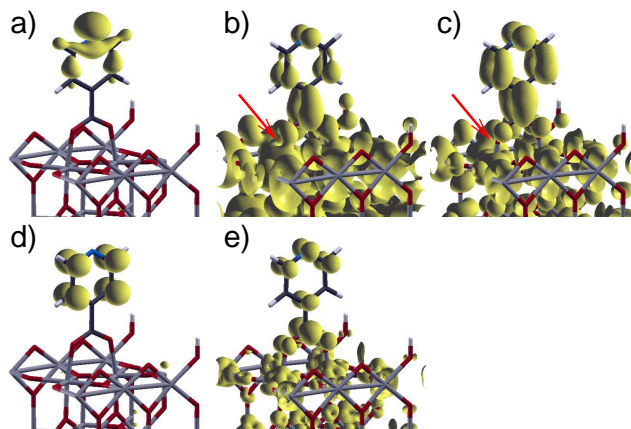


Figure 3: Local DOS corresponding to the (a) HOMO, (b-c) LUMO, (d) LUMO+1, and (e) LUMO+2 peaks in the DOS plot shown in Fig. 2. The arrows in panels (b) and (c) highlight the absence and the existence, respectively, of a nodal plane perpendicular to the Ti–O bonds, indicating the bonding/antibonding character of the substrate-molecule interaction.

(c). These values can be compared to those given by Martsinovich and Troisi.² They adopted a Hamiltonian-partitioning technique to compute the coupling elements between the molecule and substrate, and from that to obtain the lifetime for the LUMO state (taken as a whole). Their value, 0.68 ± 0.41 fs, corresponds to $\Gamma \approx 1$ eV which is consistent with the splitting between the LUMO components that we report in Fig. 2. Therefore, our calculation confirms a strong interaction between the isonicotinic acid and the TiO_2 substrate as that reported by Martsinovich and Troisi. However, our simulations also point out that such interaction cannot be interpreted solely in terms of a single resonant lifetime, since it determines a splitting of the LUMO to two components which can be pumped independently. Next, the LUMO+1 (d), which falls in a region with a small TiO_2 DOS and has no weight on the $-\text{COO}-$ termination of the molecule, shows no hybridization with the substrate, with $\Gamma = 0$. The LUMO+2 couples to substrate states, and a single peak can be identified in this case for which we obtain $\Gamma = 15$ meV ($\tau = 44$ fs). Finally, from Fig. 2 one can also notice that the adsorption does not introduce a rehybridization among molecular states, which seem well described in terms of those of the gas phase molecule. All the values of the lifetimes for the ground state molecule are collected in Fig. 1. They could refer to the lifetime of electrons either added to the system or promoted to unoccupied states from extended MOs, where the role of the electron-hole interaction is less determinant and often neglected.

Table 1: Linewidths (FWHM, Γ) and transfer time, τ , for molecular orbitals of isonicotinic acid on $\text{TiO}_2(110)$ as in a neutral and core-excited configuration.

Ground state	HOMO	LUMO (b)	LUMO (c)	LUMO+1	LUMO+2
Γ (meV)	0	80	186	0	15
τ (fs)		8	4		44
<hr/>				LUMO+1	LUMO+2
N 1s \rightarrow valence					
Γ (meV)				7	15
τ (fs)				93	44

Before considering the influence of a core-level excitation, it is worth stressing that relatively small widths, like that of the LUMO+2 state reported here, are difficult to determine from the DOS of molecules adsorbed on a slab or cluster. In such a system the states (artificially quantized in the direction perpendicular to the surface) should be dense enough to allow for working out a lorentzian profile. Consider as an example the energy window just above the conduction band edge, where the bulk DOS is about 3 states/eV/spin/unit cell (6 atoms). Hence with a (3×1) surface periodicity we need more than 50 TiO_2 trilayers to achieve an average distance between electronic levels of 2 meV, which allows obtaining five states (at each \mathbf{k}_{\parallel}) within the FWHM of a resonance with $\Gamma = 10$ meV. Thicker slabs would then be necessary for even narrower resonances.

We now turn to the case of a molecule excited by X-ray radiation. We considered excitations from the N 1s state, corresponding to a binding energy of ~ 400 eV, as occurs in experimental measurements by the core-hole-clock method.¹⁶ In the simulation, this is obtained by promoting a N 1s electron from the core to a valence state. The core-hole is included in the pseudopotential that now accounts for the interaction of valence electrons with a core-excited N 1s^{*} ion. The excited electron is explicitly included in the self-consistent calculation (so that the system remains neutral) populating the molecular LUMO and, due to the presence of the N core-hole, remains strictly localized within the molecule (see below). The additional positive nuclear charge lowers the effective potential in the molecular region, shifting the molecular orbitals to lower energies. See Fig. 4 where the corresponding projected DOS is shown. In close agreement with the experiments¹⁶ the LUMO is brought down inside the energy gap, so that no resonant charge transfer can take place from this state of the molecule with a core-excited N atom. The LUMO’s density distribution is

shown in Fig. 5(a), in which the coupling with substrate states is absent, in clear contrast with the ground-state molecule. As a consequence of the core-hole attraction, the LUMO is now polarized towards the N atom, as can be observed by comparing Fig. 5(a) with Fig. 3(b)-(c). Indeed, with respect to the MOs of the free molecule, we can appreciate some rehybridization of the states: see the LUMO and LUMO+2 peaks in Fig. 4.

At variance with the neutral-core case shown in Fig. 2, the LUMO+1 and LUMO+2 are also significantly downshifted. In particular, the LUMO+1 enters a region of large density of substrate states with which to couple, as can be seen in Fig. 5(b). We obtain a width $\Gamma = 7$ meV ($\tau = 93$ fs). Notice how the symmetry and spatial distribution of the orbital strongly influence the transfer rate. In fact the LUMO+1 of the core-excited case (Fig. 5) lies in the same energy region as the LUMO of the ground state system shown in Fig. 2, but the resonant lifetime is at least one order of magnitude larger. For the LUMO+2, whose LDOS is depicted in Fig. 5(c), one obtains coincidentally the same width as that for the neutral-core molecule ($\tau = 44$ fs), although the orbital couples to different substrate states. We mention that the HOMO, not reported here, lies at much lower energies, because of its large weight around the N atom (recall Fig. 3(a)) where the attraction by the core-hole is more effective.

Discussion

Our results, and in particular the comparison between Fig. 2 and Fig. 4, highlights the importance of excitonic effects in the calculation of the resonant lifetime, in comparing to measurements obtained with the core-hole-clock method. Excitonic effects are also important for the transfer of electrons excited by visible light, where the simplifications adopted here due to the localized character of the core-hole do not hold. Other methods, like time-dependent DFT or the two-particle Bethe-Salpeter equation could be used instead.⁵² However, the large computational cost of such approaches limits their applicability to the evaluation of optical spectra for relatively small systems,⁵³ while no implementation for semi-infinite substrates (to access transfer times) exists to the

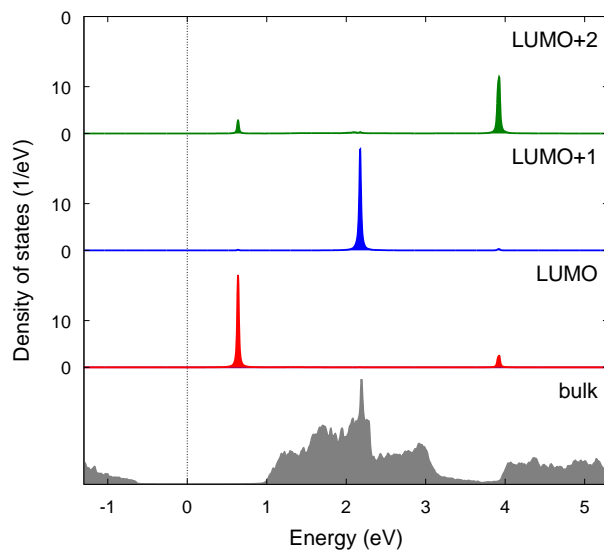


Figure 4: DOS for isonicotinic acid adsorbed on semi-infinite $\text{TiO}_2(110)$, projected on the gas-phase molecular orbitals, with a N 1s electron excited to valence. The shaded area is the bulk TiO_2 DOS. Compare with Fig. 2.

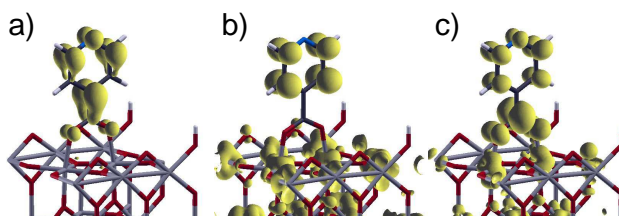


Figure 5: Local DOS corresponding to the (a) LUMO, (b) LUMO+1, and (c) LUMO+2 peaks in the DOS plot shown in Fig. 4, with N 1s electron excited to valence.

best our knowledge. Hence electron-hole interaction is most often neglected in computing resonant linewidths, as we do here for the neutral-core case.

Owing to the large excitonic effect induced by the presence of the N core-hole, the agreement of the linewidth of isonicotinic acid with the experimental one¹⁶ claimed in Ref.,² where the ground-state configuration was used, is fortuitous. Our analysis instead correctly suppresses resonant transfer from the LUMO state, and comparison to the LUMO+1 and LUMO+2 states should be done instead. For these states (especially the LUMO+2 with largest signal/noise ratio) an upper limit of 5 fs was measured.¹⁶ Since we are focusing on the resonant part of the injection process, our estimates are necessarily upper bounds of the complete (theoretical) transfer time, that will be decreased due to additional inelastic contributions (due, e.g., to electron-phonon and electron-electron interactions²³). Still, our calculated resonant charge transfer time is one order of magnitude larger than that in experiments, a discrepancy which might be due to other effects not included in our estimate, as we further discuss.

In common to most other studies in the related literature (an exception was recently given⁵⁴) our approach takes single-particle energy levels from KS eigenvalues, while DFT is a ground state theory. Luckily enough, some errors in the KS-DFT spectrum tend to cancel out. This occurs for the TiO₂ band gap and the HOMO-LUMO gap in the molecule, both being underestimated. Due to a fortuitous coincidence, the relative position of molecular and substrate states shown in Fig. 4 seems to be in rather good agreement with the one reported in the experiments in Ref.¹⁶ However, since *a priori* there is no guarantee that proper energy alignment stems from error cancellations, it is important to understand how the results depend on such alignment. For this reason, we rigidly shift the molecular orbital energies with respect to the substrate bands as a post-self-consistency correction. This is implemented by adding the energy shift $\Delta\epsilon$ to the terms of the Hamiltonian matrix belonging to the adsorbate:

$$H_{\mu\nu\mathbf{k}_{\parallel}} = H_{\mu\nu\mathbf{k}_{\parallel}} + S_{\mu\nu\mathbf{k}_{\parallel}}\Delta\epsilon, \mu, \nu \in \text{molecule}. \quad (7)$$

Next we compute the electronic structure with values of $|\Delta\epsilon|$ up to ≈ 1 eV and the corresponding lifetime of LUMO+1 and LUMO+2 states (in presence of the N 1s excitation). The results are reported in Fig. 6 as a function of the energy of the MOs, showing a moderate dependence on energy, except for the LUMO+1 at about 3 eV. According to these data, the misalignment of the MOs with respect to the TiO₂ bands does not appear to be at the origin of the large discrepancy between the measured and the calculated charge transfer times in this system. It is also interesting to note that, although the lifetimes in Fig. 6 approximately follow the profile of the TiO₂ substrate DOS, the symmetry and spatial distribution of both, the molecule and substrate states, plays a key role in determining the values of the resonant charge transfer times.

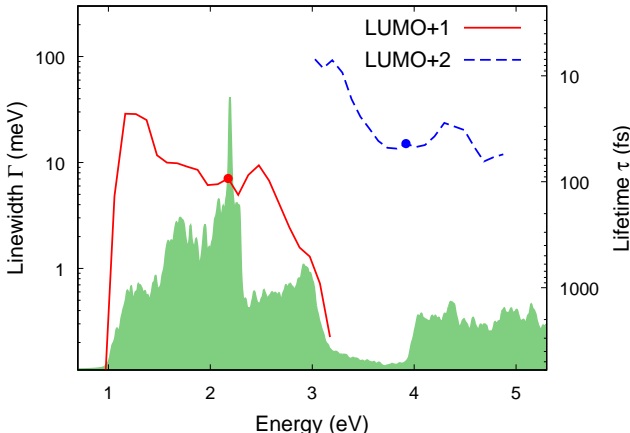


Figure 6: Linewidth and lifetime of the molecular orbitals of isonicotinic acid with one N 1s electron excited into the LUMO, as a function of the energy of the molecular orbitals. Bullets mark the self-consistent values, and the lines are the results obtained using a post-self-consistent rigid shift of the molecular Hamiltonian operated by Eq. (7). The shaded area is the bulk TiO₂ DOS.

Finally, we consider the effects of neglecting a finite temperature and those related to the use of ground state geometry. As temperature is increased, we should consider different effects induced by the dynamics of the system. First, the core-level excitation could occur for molecules in different structural configurations than the energy minimum. This could open up new decay channels which might vanish in the high-symmetry structure depicted in Fig. 1. This feature was studied extensively in various contexts, by making averages over snapshots of molecular dynamics simulations.⁵⁵ A detailed analysis in this direction goes beyond the realm of the present work. However,

as an example, we computed the effect of a rigid 30° tilt of the molecule around the [001] axis passing through the O atoms of the -COO group (which is compatible with a polar angle of $0 \pm 40^\circ$ observed experimentally⁵⁶): the coupling of the π electron system to the substrate is enhanced, resulting in a significant reduction of the LUMO+2 lifetime to about 1/3 of the calculated value for the molecule remains perpendicular to the surface. Therefore, the presence of modified geometries in which the molecule interacts more strongly with the TiO_2 substrate, might be one of the reasons behind the small charge-transfer times measured for isonicotinic acid,¹⁶ and a way to reconcile the experiment with our theoretical estimations.

Conclusions

The resonant lifetimes of the molecular states of isonicotinic molecules adsorbed on the surface of rutile $\text{TiO}_2(110)$ were evaluated from first principles. Using a Green's function based methodology we could take into account the continuum density of states of the semi-infinite substrate. This is not accessible by slab or cluster models and provides a very detailed picture of the hybridization between molecule and substrate states. For an isonicotinic acid molecule in its ground state, the Kohn-Sham LUMO resonance broadens and splits into two components, with linewidths corresponding to short lifetimes (4 and 8 fs, respectively). However, in the presence of a core-excited atom (as occurs in measurements of electron transfer by core-level spectroscopy), electron injection from the LUMO is suppressed as it enters the substrate band gap. Resonant transfer is still possible for higher lying states, for which longer times (93 fs and 44 fs for the LUMO+1 and LUMO+2, respectively) are calculated for the most stable adsorption configuration. Such values are at least one order of magnitude larger than the lifetimes of a few femtoseconds found in the experiment, which also comprise inelastic contributions (not taken into account in the present work). The dependence on the relative alignment of molecular and substrate states was investigated and demonstrated to have a moderate effect on the results reported here. We speculate that other adsorption configurations with an increased molecule/substrate interaction, different from the relaxed

ground-state geometry used here, could be abundant in the experimental situation.

Our work implements Green's function methods to the calculation of the lifetime of molecular states at an extended substrate. It highlights the importance of incorporating the excitonic effects associated with the presence of core-excited species when comparison with experimental information obtained using the core-hole-clock method is pursued. It further stresses that various types of experiments might provide contrasting charge transfer times since, in some cases, they look into very different spatial distributions and couplings to the substrate of the involved MOs.

Acknowledgement

We acknowledge support from the MIUR of Italy through PRIN project DSSCX (n. 20104XET32). Computational resources were made available in part by CINECA (application code HP10C0TP0R). CM thanks CARIPLO Foundation for its support within the PCAM European Doctoral Programme and Pirelli Corimav for his PhD scholarship. DSP acknowledges support the Basque Departamento de Educación, UPV/EHU (Grant No. IT-366-07), the Spanish Ministerio de Ciencia e Innovación (Grant No. FIS2010-19609-C02-02), the ETORTEK program funded by the Basque Departamento de Industria and the Diputación Foral de Guipuzcoa, the EU through the FP7 PAMS project and the German DFG through SFB 1083.

References

- (1) Grätzel, M. Dye-sensitized solar cells. *J. Photochem. Photobiol. C Photochem. Rev.* **2003**, *4*, 145–153.
- (2) Martsinovich, N.; Troisi, A. High-Throughput Computational Screening of Chromophores for Dye-Sensitized Solar Cells. *J. Phys. Chem. C* **2011**, *115*, 11781–11792.
- (3) Listorti, A.; O'Regan, B.; Durrant, J. R. Electron Transfer Dynamics in Dye-Sensitized Solar Cells. *Chem. Mater.* **2011**, *23*, 3381–3399.

- (4) Hardin, B. E.; Snaith, H. J.; McGehee, M. D. The renaissance of dye-sensitized solar cells. *Nat. Photonics* **2012**, *6*, 162–169.
- (5) Brühwiler, P. A.; Karis, O.; Mårtensson, N. Charge-transfer dynamics studied using resonant core spectroscopies. *Rev. Mod. Phys.* **2002**, *74*, 703–740.
- (6) Menzel, D. Ultrafast charge transfer at surfaces accessed by core electron spectroscopies. *Chem. Soc. Rev.* **2008**, *37*, 2212.
- (7) Wurth, W.; Menzel, D. Ultrafast electron dynamics at surfaces probed by resonant Auger spectroscopy. *Chem. Phys.* **2000**, *251*, 141–149.
- (8) Hannappel, T.; Burfeindt, B.; Storck, W.; Willig, F. Measurement of Ultrafast Photoinduced Electron Transfer from Chemically Anchored Ru-Dye Molecules into Empty Electronic States in a Colloidal Anatase TiO₂ Film. *J. Phys. Chem. B* **1997**, *101*, 6799–6802.
- (9) Ino, D.; Watanabe, K.; Takagi, N.; Matsumoto, Y. Electron Transfer Dynamics from Organic Adsorbate to a Semiconductor Surface: Zinc Phthalocyanine on TiO₂ (110). *J. Phys. Chem. B* **2005**, *109*, 18018–18024.
- (10) Bronner, C.; Schulze, M.; Hagen, S.; Tegeder, P. The influence of the electronic structure of adsorbate-substrate complexes on photoisomerization ability. *New J. Phys.* **2012**, *14*, 043023.
- (11) Rudolf, P.; Golden, M. S.; Brühwiler, P. A. Studies of fullerenes by the excitation, emission, and scattering of electrons. *J. Electron Spectrosc. Relat. Phenom.* **1999**, *100*, 409–433.
- (12) Hill, I. G.; Kahn, A.; Cornil, J.; dos Santos, D. A.; Brédas, J. L. Occupied and unoccupied electronic levels in organic π -conjugated molecules: comparison between experiment and theory. *Chem. Phys. Lett.* **2000**, *317*, 444–450.
- (13) Kong, L.; Perez Medina, G. J.; Colón Santana, J. A.; Wong, F.; Bonilla, M.; Colón Amill, D. A.; Rosa, L. G.; Routaboul, L.; Braunstein, P.; Doudin, B.; et al., Weak screening of a large dipolar molecule adsorbed on graphene. *Carbon* **2012**, *50*, 1981–1986.

- (14) Fölisch, A.; Feulner, P.; Hennies, F.; Fink, A.; Menzel, D.; Sanchez-Portal, D.; Echenique, P. M.; Wurth, W. Direct observation of electron dynamics in the attosecond domain. *Nature* **2005**, *436*, 373–376.
- (15) Schnadt, J.; Brühwiler, P. A.; Patthey, L.; O’Shea, J. N.; Södergren, S.; Odelius, M.; Ahuja, R.; Karis, O.; Bäessler, M.; Persson, P.; et al., Experimental evidence for sub-3-fs charge transfer from an aromatic adsorbate to a semiconductor. *Nature* **2002**, *418*, 620–623.
- (16) Schnadt, J.; O’Shea, J. N.; Patthey, L.; Kjeldgaard, L.; Åhlund, J.; Nilson, K.; Schiessling, J.; Krempaský, J.; Shi, M.; Karis, O.; et al., Excited-state charge transfer dynamics in systems of aromatic adsorbates on TiO₂ studied with resonant core techniques. *J. Chem. Phys.* **2003**, *119*, 12462.
- (17) Batra, A.; Kladnik, G.; Vázquez, H.; Meisner, J. S.; Floreano, L.; Nuckolls, C.; Cvetko, D.; Morgante, A.; Venkataraman, L. Quantifying through-space charge transfer dynamics in π -coupled molecular systems. *Nat. Commun.* **2012**, *3*, 1086.
- (18) Martsinovich, N.; Troisi, A. Theoretical studies of dye-sensitized solar cells: from electronic structure to elementary processes. *Energy Environ. Sci.* **2011**, *4*, 4473.
- (19) Le Bahers, T.; Pauporté, T.; Lainé, P. P.; Labat, F.; Adamo, C.; Ciofini, I. Modeling Dye-Sensitized Solar Cells: From Theory to Experiment. *J. Phys. Chem. Lett.* **2013**, *4*, 1044–1050.
- (20) Stier, W.; Prezhdo, O. V. Nonadiabatic Molecular Dynamics Simulation of Light-Induced Electron Transfer from an Anchored Molecular Electron Donor to a Semiconductor Acceptor. *J. Phys. Chem. B* **2002**, *106*, 8047–8054.
- (21) Duncan, W. R.; Prezhdo, O. V. Theoretical Studies of Photoinduced Electron Transfer in Dye-Sensitized TiO₂. *Annu. Rev. Phys. Chem.* **2007**, *58*, 143–184.

- (22) Chulkov, E. V.; Kliewer, J.; Berndt, R.; Silkin, V. M.; Hellsing, B.; Crampin, S.; Echenique, P. M. Hole dynamics in a quantum-well state at Na/Cu(111). *Phys. Rev. B* **2003**, *68*, 195422.
- (23) Achilli, S.; Butti, G.; Trioni, M. I.; Chulkov, E. V. Electronic structure and lifetime broadening of a quantum-well state on $p(2 \times 2)$ K/Cu(111). *Phys. Rev. B* **2009**, *80*, 195419.
- (24) Häming, M.; Schöll, A.; Umbach, E.; Reinert, F. Adsorbate-substrate charge transfer and electron-hole correlation at adsorbate/metal interfaces. *Phys. Rev. B* **2012**, *85*, 235132.
- (25) Persson, P.; Lunell, S.; Brühwiler, P. A.; Schnadt, J.; Södergren, S.; O'Shea, J. N.; Karis, O.; Siegbahn, H.; Mårtensson, N.; Bässler, M.; et al., N 1s x-ray absorption study of the bonding interaction of bi-isonicotinic acid adsorbed on rutile TiO₂(110). *J. Chem. Phys.* **2000**, *112*, 3945.
- (26) Persson, P.; Lundqvist, M. J.; Ernstorfer, R.; Goddard, W. A.; Willig, F. Quantum Chemical Calculations of the Influence of Anchor-Cum-Spacer Groups on Femtosecond Electron Transfer Times in Dye-Sensitized Semiconductor Nanocrystals. *J. Chem. Theory Comput.* **2006**, *2*, 441–451.
- (27) Kondov, I.; Cizek, M.; Benesch, C.; Wang, H.; Thoss, M. Quantum Dynamics of Photoinduced Electron-Transfer Reactions in Dye-Semiconductor Systems: First-Principles Description and Application to Coumarin 343-TiO₂. *J. Phys. Chem. C* **2007**, *111*, 11970–11981.
- (28) Labat, F.; Ciofini, I.; Hratchian, H. P.; Frisch, M.; Raghavachari, K.; Adamo, C. First Principles Modeling of Eosin-Loaded ZnO Films: A Step toward the Understanding of Dye-Sensitized Solar Cell Performances. *J. Am. Chem. Soc.* **2009**, *131*, 14290–14298.
- (29) Brivio, G. P.; Butti, G.; Caravati, S.; Fratesi, G.; Trioni, M. I. Theoretical approaches in adsorption: alkali adatom investigations. *J. Phys. Condens. Matter* **2007**, *19*, 305005.
- (30) Inglesfield, J. E. A method of embedding. *J. Phys. C Solid State Phys.* **1981**, *14*, 3795–3806.

- (31) Brivio, G. P.; Trioni, M. I. The adiabatic molecule-metal surface interaction: Theoretical approaches. *Rev. Mod. Phys.* **1999**, *71*, 231.
- (32) Achilli, S.; Trioni, M. I.; Brivio, G. P. Detailed features of the surface electronic states of K/Cu(111) by density functional theory. *Phys. Rev. B* **2010**, *81*, 165444.
- (33) Trioni, M. I.; Achilli, S.; Chulkov, E. V. Key ingredients of the alkali atom - metal surface interaction: Chemical bonding versus spectral properties. *Prog. Surf. Sci.* **2013**, *88*, 160–170.
- (34) Sánchez-Portal, D.; Menzel, D.; Echenique, P. First-principles calculation of charge transfer at surfaces: The case of core-excited Ar*(2p_{3/2}-14s) on Ru(0001). *Phys. Rev. B* **2007**, *76*, 235406–235424.
- (35) Sánchez-Portal, D. Slab calculations and Green's function recursive methods combined to study the electronic structure of surfaces: application to Cu(111)-(4×4)-Na. *Prog. Surf. Sci.* **2007**, *82*, 313–335.
- (36) Brandbyge, M.; Mozos, J.-L.; Ordejón, P.; Taylor, J.; Stokbro, K. Density-functional method for nonequilibrium electron transport. *Phys. Rev. B* **2002**, *65*, 165401.
- (37) Rocha, A. R.; García-suárez, V. M.; Bailey, S. W.; Lambert, C. J.; Ferrer, J.; Sanvito, S. Towards molecular spintronics. *Nat. Mater.* **2005**, *4*, 335–339.
- (38) Kim, Y.-H.; Tahir-Kheli, J.; Schultz, P.; Goddard, W. First-principles approach to the charge-transport characteristics of monolayer molecular-electronics devices: Application to hexanedithiolate devices. *Phys. Rev. B* **2006**, *73*, 235419.
- (39) Palacios, J. J.; Pérez-Jiménez, A. J.; Louis, E.; SanFabián, E.; Vergés, J. A.; García, Y. Molecular electronics with Gaussian98/03. *Comput. Chem. Rev. Curr. Trends* **2005**, *9*, 1.
- (40) Triguero, L.; Pettersson, L. G. M.; Ågren, H. Calculations of near-edge x-ray-absorption spectra of gas-phase and chemisorbed molecules by means of density-functional and transition-potential theory. *Phys. Rev. B* **1998**, *58*, 8097.

- (41) Prendergast, D.; Galli, G. X-Ray Absorption Spectra of Water from First Principles Calculations. *Phys. Rev. Lett.* **2006**, *96*, 215502.
- (42) Soler, J. M.; Artacho, E.; Gale, J. D.; García, A.; Junquera, J.; Ordejón, P.; Sánchez-Portal, D. The SIESTA method for ab initio order- N materials simulation. *J. Phys. Condens. Matter* **2002**, *14*, 2745–2779.
- (43) Nitzan, A. *Chemical dynamics in condensed phases relaxation, transfer and reactions in condensed molecular systems*; Oxford University Press, 2006.
- (44) Chambers, S.; Thevuthasan, S.; Kim, Y. J.; Herman, G. S.; Wang, Z.; Tober, E.; Ynzunza, R.; Morais, J.; Peden, C. H. F.; Ferris, K.; et al., Chemisorption geometry of formate on Ti₂(110) by photoelectron diffraction. *Chem. Phys. Lett.* **1997**, *267*, 51–57.
- (45) Fukui, K.; Onishi, H.; Iwasawa, Y. Imaging of individual formate ions adsorbed on TiO₂(110) surface by non-contact atomic force microscopy. *Chem. Phys. Lett.* **1997**, *280*, 296–301.
- (46) Bates, S. P.; Kresse, G.; Gillan, M. J. The adsorption and dissociation of ROH molecules on TiO₂(110). *Surf. Sci.* **1998**, *409*, 336–349.
- (47) Perdew, J. P.; Burke, K.; Ernzerhof, M. Generalized gradient approximation made simple. *Phys. Rev. Lett.* **1996**, *77*, 3865.
- (48) Junquera, J.; Zimmer, M.; Ordejón, P.; Ghosez, P. First-principles calculation of the band offset at BaO/BaTiO₃ and SrO/SrTiO₃ interfaces. *Phys. Rev. B* **2003**, *67*, 155327.
- (49) Mauri, F.; Car, R. First-Principles Study of Excitonic Self-Trapping in Diamond. *Phys. Rev. Lett.* **1995**, *75*, 3166–3169.
- (50) Arntz, F.; Yacoby, Y. Electroabsorption in Rutile (TiO₂). *Phys. Rev. Lett.* **1966**, *17*, 857–860.
- (51) Hammer, B.; Nørskov, J. K. In *Theoretical surface science and catalysis-calculations and concepts*; Elsevier, 2000; Vol. 45, pp 71–129.

- (52) Onida, G.; Reining, L.; Rubio, A. Electronic excitations: density-functional versus many-body Green's-function approaches. *Rev. Mod. Phys.* **2002**, *74*, 601–659.
- (53) De Angelis, F.; Fantacci, S.; Selloni, A. Alignment of the dye's molecular levels with the TiO₂ band edges in dye-sensitized solar cells: a DFT-TDDFT study. *Nanotechnology* **2008**, *19*, 424002.
- (54) Umari, P.; Giacomazzi, L.; De Angelis, F.; Pastore, M.; Baroni, S. Energy-level alignment in organic dye-sensitized TiO₂ from GW calculations. *J. Chem. Phys.* **2013**, *139*, 014709.
- (55) De Angelis, F.; Fantacci, S.; Gebauer, R. Simulating Dye-Sensitized TiO₂ Heterointerfaces in Explicit Solvent: Absorption Spectra, Energy Levels, and Dye Desorption. *J. Phys. Chem. Lett.* **2011**, *2*, 813–817.
- (56) Schnadt, J.; Schiessling, J.; O'Shea, J. N.; Gray, S. M.; Patthey, L.; Johansson, M. K.-J.; Shi, M.; Krempaský, J.; Åhlund, J.; Karlsson, P. G.; et al., Structural study of adsorption of isonicotinic acid and related molecules on rutile TiO₂(110) Ir: XAS and STM. *Surf. Sci.* **2003**, *540*, 39–54.